Chem. Chem. Technol., 2025,
Vol. 19, No. 2, pp. 196–213

Chemistry

CRYSTAL STRUCTURE AND PROPERTIES OF STRONTIUM COBALT VANADATE CERAMICS FOR MICROWAVE APPLICATIONS

***Viktor Zavodyannyi*[1,✉], *Mykola Voloshyn*[1], *Valentina Zubenko*[1], *Roman Kovalenko*[1], *Iryna Bereziuk*[2]**

https://doi.org/10.23939/chcht19.02.196

Abstract. The development of next-generation cellular communications requires materials with high dielectric properties at high frequencies. $SrCoV_2O_7$, ceramics, synthesized using Ultra Low-Temperature Co-Fired Ceramic (ULTCC) technology, offer promising characteristics. This study analyzed their crystal structure using X-ray diffraction, SEM microscopy, and energy dispersive spectroscopy. The results confirmed a single-phase monoclinic structure (P 1 21/c 1) with lattice parameters a=6.8360(7) Å, b=14.823(2) Å, c=11.271(1) Å, β=99.4610(5)°. The material exhibits potential for microwave applications, including resonators, antennas, and filters, due to its dielectric properties and compatibility with aluminium electrodes.

Keywords: breg-Brentano survey geometry, Rietveld method, low-temperature synthesis, thermal conductivity, dielectrics, sintering.

1. Introduction

Materials that retain their stability at low temperatures are classified as Ultra Low-Temperature Co-Fired Ceramic (ULTCC). Such materials are used in aerospace, electronics, oil and gas, and medical applications due to their unique properties: high mechanical strength, resistance to temperature fluctuations, and good electrical, chemical, and thermal conductivity. The Ultra Low-Temperature Co-Fired Ceramic technology is an important tool for the manufacture of microwave dielectrics, ceramic chips and multilayer devices, including mobile communications, Wi-Fi, Bluetooth and fifth-generation wireless networks. As noted by Ahmed *et al.*[1], the growing demand for wireless communications and the congestion of the 3 GHz spectrum is leading to the need to switch to millimetre waves with a frequency range of 30–300 GHz, which offer a wide range for future wireless communication systems. The efficient use of these high-frequency bands requires the latest materials with high microwave properties and a low-temperature coefficient of frequency (τf), which is critical for applications in 5G and other millimetre wave technologies. In recent years, research efforts have been focused on finding materials with a sintering temperature of 600 °C and below that are compatible with aluminium electrodes.

Recently, several new ceramic materials have been developed for use in ULTCC, which provide high efficiency in microwave systems. For example, Varghese *et al.*[2] in presented ULTCC materials with a sintering temperature of 400 °C for the first time. In addition, Liu *et al.*[3] doped BaV_2O_6-based ceramics with LiF, demonstrating a significant increase in the quality factor, reaching 16.800 GHz at a sintering temperature of 475 °C, which is 5.6 times higher than that of pure BaV_2O_6. Deng *et al.*[4] doped $Ba_3V_2O_8$ ceramics with Li_2CO_3, demonstrating excellent microwave properties, reducing the sintering temperature to 660 °C and reaching $Q\times f$=33.000 GHz and τf=13 ppm/°C. The choice of lithium-salt additives for ceramics, such as $LiCo_{1-x}A_xVO_4$, provided high microwave performance in the study by Huang *et al.*[5].

It is particularly important to develop materials for co-combustion with aluminium electrodes, which increases their stability and compatibility with existing technologies. Vanadate-based compounds, such as $SrCoV_2O_7$, show promise for use in high-tech dielectric materials. It is known that such compounds exhibit good microwave characteristics: high dielectric constant, low energy loss, and stability in different temperature regimes. According to the results presented by Suresh and Ratheesh[6], $SrZnV_2O_7$ ceramics sintered at 660 °C demonstrated excellent microwave properties with εr=10.2, $Q\times f$=31.900 GHz, τf=–76 ppm/°C, and good chemical compatibility with aluminium and silver electrodes. In addition, the study by Huang *et al.*[7] of

[1] Department of Hydraulic Engineering, Water and Electrical Engineering, Kherson State Agrarian and Economic University, Kropyvnytskyi, Ukraine
[2] Department of Automation of Production Processes, Central Ukrainian National Technical University, Kropyvnytskyi, Ukraine
✉ *zavodyannyiviktor@gmail.com*

$(Mg_{1-x}Zn_x)V_2O_6$ ceramics revealed a significant improvement in microwave properties when using Zn instead of Mg, which allowed achieving high $Q \times f$ values (up to 15.300 GHz) and almost zero temperature frequency coefficient ($\tau f \approx -3.4$ ppm/°C).

Recent studies demonstrate a variety of approaches to creating materials with high microwave performance for ULTCC technologies and 5G applications. For example, as noted by Zou *et al.*[8], a Li_2O-Al_2O_3-B_2O_3-based glass-ceramic with 4 mol. % Al_2O_3 added, sintered at 650 °C, showed excellent microwave properties, which indicates its promise. Another example is the work of Yu *et al.*[9], where $ATeMoO_6$ (*A*=Mg, Zn) ceramics sintered at 660 °C and 650 °C showed high $Q \times f$ values up to 34.453 GHz with good chemical stability.

However, despite the significant progress in the study of low-temperature ceramics, there are still unresolved problems that limit its further implementation in high-tech industries. For the $SrCoV_2O_7$ compound, which demonstrates promising dielectric properties, there is no detailed data on the crystal structure and microstructural parameters. It is not known how defects, such as vacancies or the inter-nodal arrangement of atoms, affect the physical and chemical properties of the material, including its thermal conductivity, dielectric constant, and stability at high temperatures. The study of these aspects is important for optimizing ceramic parameters, ensuring its technological compatibility with modern manufacturing methods, such as the use of aluminium electrodes, and improving its performance for use in microwave devices and ULTCC technologies. The study aims to analyze the crystal structure and microstructural parameters of $SrCoV_2O_7$ to determine their influence on the functional properties of the material and develop recommendations for its use in high-tech devices.

2. Experimental

2.1. Materials

To study the crystal structure of $SrCoV_2O_7$ ceramics and its properties, the methods of synthesis and X-ray diffraction analysis were used, which provided high accuracy in determining the phase composition and parameters of the crystal lattice.

During the study, one of the key stages was the preparation of high-quality samples to ensure the reliability of the study results. The samples for obtaining the diffractogram were prepared by solid-phase sintering, the process is described in detail in Y.–T. Huang *et al.* Highly pure reagents (>99.9 %, Alfa Aesar, USA) were used to prepare the samples: $SrCO_3$, CoO, MgO, and V_2O_5. The required amounts of each component were calculated based on stoichiometric ratios to ensure the formation of a phase composition corresponding to $SrCoV_2O_7$. Subsequently, the reagents were mixed and ground in distilled water using a ball mill.

The reagents were mixed and ground in a planetary ball mill for 24 hours with a material-to-ball ratio of 1:10. The balls used in the grinding process were made of zirconia to minimize contamination, and the inner surface of the mill drum was lined with zirconia as well. This choice was made to avoid any potential contamination from materials like aluminum oxide, which could significantly affect the phase composition of the resulting material, especially if corundum balls had been used. To ensure the integrity of the mixture and to monitor for any potential contamination, the presence of foreign impurities was regularly checked during the study. Specifically, X-ray phase analysis was performed on the ground mixture to detect any unintentional contaminants. The analysis confirmed that the phase composition of the material remained consistent with the expected results, without any significant foreign impurities from the grinding process.

To ensure particle size control, laser diffraction was used, which confirmed an average particle size of 1–3 μm. This particle size range was selected based on both previous studies and literature, where finer particle sizes (1–3 μm) have been shown to enhance the sintering process and improve the homogeneity of phase composition in ceramic materials[10]. This range also plays a crucial role in achieving desirable physical and mechanical properties in ceramics, such as increased density, phase purity, and structural integrity. Moreover, smaller particles provide a higher surface area for sintering, contributing to improved electrical and dielectric properties, which are essential for microwave applications.

After grinding, the resulting mixture was dried in a vacuum dryer at 80 °C and then calcined in a muffle furnace at 570 °C for 2 hours. This step was necessary to remove volatile components and promote preliminary reaction between the oxides. The powder obtained after calcination was re-grounded with the addition of polyvinyl alcohol. The polyvinyl alcohol was used as a binder to improve the moulding of the samples. Afterwards, the mixed powder was compressed into cylindrical tablets of 11 mm diameter and 5 mm height at 20 MPa in stainless steel dies. The resulting "green" cylinders were 5 mm high and 11 mm in diameter.

2.2. Methods

The pre-formed tablets were sintered in an oven within a temperature range of 600 °C to 690 °C for a duration of 4 hours. This temperature range was selected based on previous studies indicating that sintering within

this range is optimal for achieving a homogeneous phase composition and stability in $SrCoV_2O_7$ ceramics. The choice of this temperature range was further supported by research on similar microwave dielectric materials, such as the $SrZnV_2O_7$ ceramics, which demonstrated excellent microwave properties when sintered at temperatures around 660 °C[9]. Additionally, the holding time of 4 hours was optimized to ensure sufficient diffusion and phase stabilization, as well as to prevent defects that might occur with insufficient sintering time.

This sintering duration was chosen based on the successful results of other studies, where a similar duration was employed to achieve optimal structural integrity and dielectric properties[9]. The heating rate of 5 °C per minute was selected to avoid thermal stresses and to ensure the gradual and uniform heating of the material. Cooling was performed together with the furnace to minimize the formation of thermal cracks, ensuring the mechanical stability of the samples post-sintering.

The crystal structure was analyzed by X-ray diffraction. The X-ray diffraction analysis was performed on a diffractometer (Rigaku SmartLab) with a copper anode (Cu Kα=1.5406 Å). Spectra were recorded in the 2θ range from 10° to 80° at a scan rate of 0.02° per second. The calibration was performed using the LaB_6 standard. Following published data[10], the diffraction spectrum of the obtained compound was in good agreement with the spectrum from the ICDD PDF No. 00-044-0455 database, which confirmed the success of the synthesis. The spectrum from the ICDD database under the number 00-044-0455 was used for further studies of the crystal structure. The applied methods provided high-quality $SrCoV_2O_7$ samples suitable for further structural analysis and confirmation of phase characteristics.

3. Results and Discussion

Materials that combine the properties of transition metals and oxygen coordination polymers are attracting considerable attention in modern science. The $SrCoV_2O_7$ compound is one of such materials characterized by unique structural and physical properties. In this work, this compound was synthesized, and its crystal structure was investigated in detail. The experimental analysis was based on the method of powder X-ray diffraction in the Bragg – Brentano geometry, which uses copper-filtered radiation.

As a result of the X-ray diffraction analysis by the Rietveld method, a model of the crystal structure of $SrCoV_2O_7$ was proposed and refined. The study determined that the structure of the material is characterized by a monoclinic crystal lattice with parameters: a=6.8359(7) Å, b=14.822(2) Å, c=11.272(1) Å, and an interplanar angle β=99.461(5)°. The Rietveld method significantly improved the accuracy of the structure description, as it involves minimizing the discrepancy between the experimental and calculated diffraction spectra. Reducing the discrepancies provides a reliable refinement of lattice parameters and atomic positions. This method is especially effective for analyzing structures with possible defects that are common in oxide materials, such as partial filling of nodes, vacancies, or other microstructural anomalies.

Thus, in this case, the results showed a high correspondence between the experimental and theoretical data, which is confirmed by the value of the discrepancy factor, where R=8.81 %, indicating the high accuracy of the obtained model. This indicates that the structure of $SrCoV_2O_7$ was described in detail, and the analysis methodology is correct and effective. The proposed model made it possible to consider microstructural defects and clarify the coordination features of atoms in the crystal lattice.

The analysis of the Wickhoff coordinates and occupancy factors (s.o.f.) for Sr, Co, V and O atoms showed that oxygen atoms are central in the formation of coordination polyhedra (data are given in Table 1). The shortest distances between atoms confirm the presence of strong interatomic interactions. For the O_1 atom, the shortest distance to the Sr_4 atom is 0.724 Å, and to the Co_4 atom, this distance is 1.342 Å. Such short distances indicate strong ionic bonds that stabilize the structure. The coordination polyhedra VO_6 and CoO_6, formed by vanadium and cobalt atoms, respectively, form the basis of the crystal lattice.

Further analysis of the diffraction spectrum confirmed that the structure of $SrCoV_2O_7$ is characterized by the partial filling of the crystal lattice units, indicating the presence of microstructural defects. The main reasons for this phenomenon are vacancies, inter-nodal arrangement of atoms, and temperature effects that affect the structural and functional properties of the material.

Vacancies occur when certain ions leave their nodes in the crystal lattice, creating empty positions. For example, in the structure of $SrCoV_2O_7$, this can manifest itself in the form of the absence of strontium or oxygen ions, which disrupts the regularity of the coordination grid. In the studied structure, the factor indicating such defects is the observed change in the intensity of diffraction peaks in the (0, 4, 2) plane with an interplanar distance d=3.084 Å. The decrease in intensity may indicate local irregularities in the arrangement of atoms caused by vacancies.

Table 1. Microstructural parameters of the crystal lattice of $SrCoV_2O_7$ compound

Atom	Wyck.	s.o.f.	x	y	z
Sr_1	4e	0.209275	0.122155	0.120414	0.501564
Sr_2	4e	0.179399	0.527571	0.256404	0.648855
Sr_3	4e	0.161539	0.196746	0.675759	0.553697
Sr_4	4e	0.200287	0.497180	0.247762	0.272866
Sr_5	4e	0.119012	-0.292797	0.610710	0.134164
Sr_6	4e	0.247295	0.176112	0.484347	0.755804
Sr_7	4e	0.132500	0.381970	0.392113	0.480994
Co_1	4e	0.227362	-0.148564	0.200724	0.362482
Co_2	4e	0.252782	0.812891	0.409631	0.218081
Co_3	4e	0.207946	0.089734	0.105817	0.408612
Co_4	4e	0.258264	0.229317	0.217403	0.784409
Co_5	4e	0.303197	0.147336	0.926097	0.024523
V_1	4e	0.147500	0.896313	0.454253	0.646762
V_2	4e	0.286431	0.308685	0.298554	0.455740
V_3	4e	0.604371	0.544907	0.117759	0.482428
V_4	4e	0.314630	0.818972	0.169760	0.018566
V_5	4e	0.208603	0.233149	0.226834	0.204066
V_6	4e	0.370642	0.639161	0.522808	0.655132
V_7	4e	0.411971	0.904795	0.806300	0.844715
O_1	4e	0.426800	0.583291	0.780079	0.236911
O_2	4e	0.837270	0.533077	0.514067	0.194325
O_3	4e	1.000000	0.150003	0.894127	0.577588
O_4	4e	1.000000	0.722604	0.617851	0.477169
O_5	4e	0.732981	0.704486	0.512678	0.794586
O_6	4e	1.000000	0.922533	0.273563	0.250789
O_7	4e	1.000000	0.670331	0.444392	0.208873
O_8	4e	1.000000	0.663114	0.399992	0.538955
O_9	4e	1.000000	0.120972	0.073114	0.656842
O_{10}	4e	0.754000	0.168091	0.331908	0.031907

The interstitial arrangement of atoms implies that individual atoms occupy intermediate positions between lattice nodes. In the case of $SrCoV_2O_7$, this applies to cobalt or vanadium atoms, which can remain in energetically favourable intermediate positions during the synthesis process due to the non-equilibrium nature of cooling. Such defects not only disrupt the coordination of CoO_6 and VO_6 polyhedra but also reduce the overall density of the material. This is manifested by the observed deviations between the experimental and theoretically calculated values of diffraction peaks for certain planes, in particular (2, 0, 1).

Temperature effects also affect the orderliness of the structure, as an increase in temperature during the synthesis of the material increases the mobility of atoms. For example, under conditions of high temperature sintering in $SrCoV_2O_7$, this leads to partial desorption of oxygen and displacement of strontium atoms from their nodes, causing vacancies or inter-nodal arrangement. Additionally, this is confirmed by the values of the mismatch factor R=8.81 %. Defects affect not only the symmetry of the crystal lattice but also its physical and chemical properties. For example, oxygen vacancies in CoO_6 polyhedra reduce the electrical conductivity due to a deterioration in the efficiency of charge transfer between coordination centres. Similarly, irregularities in the nodes caused by the inter-nodal arrangement of vanadium atoms can reduce thermal conductivity due to local phonon scattering.

The proposed crystal structure model considers the above factors. For this purpose, the values of diffraction angles 2θ, interplanar distances d and peak intensities were calculated. The data compared with the obtained experimental data and reference values from the ICDD database are given in Table 2.

For one of the most intense peaks at 2θ=28.9281°, the calculated value of the interplane distance is d=3.084 Å, which corresponds to the plane with indices (0, 4, 2). Similarly, for less intense peaks, high accuracy of the results is observed: for 2θ=9.9313°, the calculated d=8.899 Å, and the experimental d=8.908 Å; for 2θ=31.1936°, the calculated value **d=2.865 Å corresponds to the experimental d=2.862 Å. The high agreement between the calculated and experimental values confirms the correctness of the proposed model and the reliability of the analysis.

Table 2. Calculated values (angle 2θ, interplanar distances and relative intensities) and reduced to ICDD for the compound $SrCoV_2O_7$

	$2\theta_{cal}$	$2\theta_{obc}$	d_{cal}	d_{obs}	I_{cal}	I_{obs}	H	K	L
1	2	3	4	5	6	7	8	9	10
1	9.9313	9.921(6)	8.89915	8.90841	2.68	1.01	0	1	–1
2	9.9313		8.89915		2.68		0	1	1
3	11.9259	11.936(1)	7.41488	7.40888	1.04	5.87	0	2	0
4	13.1136		6.74588		0.18		1	0	0
5	14.3455	14.339(3)	6.16922	6.17184	1.02	2.00	0	2	–1
6	14.3455		6.16922		1.02		0	2	1
7	14.4138		6.14015		6.21		1	1	0
8	15.3929	15.401(2)	5.75173	5.74874	1.64	2.98	1	1	–1
9	15.9243	15.932(7)	5.56096	5.55814	0.38	1.01	0	0	2
10	17.0155	17.030(7)	5.20672	5.20241	0.17	1.00	0	1	–2
11	17.0155		5.20672		0.17		0	1	2
12	17.4987		5.06403		6.10		1	1	1
13	17.7632	17.750(7)	4.98920	4.99291	2.56	1.01	1	2	0
14	18.5709	18.572(2)	4.77398	4.77374	7.81	3.97	1	2	–1
15	18.9261	18.935(3)	4.68519	4.68295	0.08	2.99	1	0	–2
16	19.6401		4.51644		0.17		0	3	–1
17	19.6401		4.51643		0.17		0	3	1
18	19.8579		4.46740		2.15		1	1	–2
19	19.9439	19.955(2)	4.44832	4.44586	0.21	3.98	0	2	–2
20	19.9439		4.44832		0.21		0	2	2
21	20.3600		4.35835		0.11		1	2	1
22	22.2823	22.28(2)	3.98651	3.98757	7.80	5.75	1	3	0
23	22.3124	22.36(3)	3.98119	3.97338	0.21	2.65	1	0	2
24	22.4311	22.45(2)	3.96039	3.95640	5.38	3.04	1	2	–2
25	22.9374		3.87412		0.03		1	3	–1
26	23.1137	23.116(3)	3.84496	3.84452	1.38	2.86	1	1	2
27	23.9892		3.70657		1.16		0	4	0
28	24.0728		3.69390		0.18		0	3	–2
29	24.0728		3.69389		0.18		0	3	2
30	24.4218	24.439(9)	3.64188	3.63942	0.13	0.98	1	3	1
31	24.7373	24.747(1)	3.59615	3.59481	10.13	9.75	0	1	–3
32	24.7373		3.59615		10.13		0	1	3
33	25.3079	25.33(3)	3.51635	3.51316	2.01	1.67	0	4	–1
34	25.3079		3.51635		2.01		0	4	1
35	25.3743	25.39(2)	3.50731	3.50487	4.92	2.80	1	2	2
36	26.1362	26.147(1)	3.40677	3.40537	11.41	12.53	1	1	–3
37	26.1895		3.39995		0.07		1	3	–2
38	26.4087	26.404(2)	3.37222	3.37275	9.21	4.93	2	0	0
39	26.8698	26.881(3)	3.31539	3.31404	9.47	15.65	0	2	–3
40	26.8698		3.31539		9.47		0	2	3
41	26.9944		3.30037		4.10		2	1	–1
42	27.0961	27.01(1)	3.28821	3.29889	0.16	4.17	2	1	0
43	27.4359	27.435(4)	3.24826	3.24842	4.41	2.05	1	4	0
44	27.9775	27.974(6)	3.18659	3.18702	0.03	2.73	1	4	–1
45	28.1701	28.160(3)	3.16524	3.16638	10.26	4.97	1	2	–3
46	28.5906	28.582(2)	3.11963	3.12053	16.10	11.53	2	0	–2

Continuation of **Table 2**

1	2	3	4	5	6	7	8	9	10
47	28.7737	28.85(3)	3.10020	3.09170	1.66	18.96	1	3	2
48	28.9281	28.9281	3.08401		100.00		0	4	–2
49	28.9281	28.9281	3.08401	3.08481	100.00	100.00	0	4	2
50	29.0680	28.97(1)	3.06948	3.07922	41.39	57.00	2	2	–1
51	29.2231	29.01(8)	3.05354	3.07540	3.58	10.06	2	2	0
52	29.2306		3.05277		1.31		1	4	1
53	29.5135	29.51(1)	3.02415	3.02490	1.00	10.63	2	1	–2
54	29.9419	29.55(2)	2.98185	3.02058	13.29	4.63	2	1	1
55	30.1133	29.952(3)	2.96527	2.98091	7.21	4.07	1	1	3
56	30.1133		2.96527		0.52		0	3	–3
57	30.7352		2.90667		0.52		0	3	3
58	31.0785	30.732(3)	2.87534	2.90693	3.44	4.09	1	4	–2
59	31.1936	31.079(7)	2.86499	2.87532	7.92	5.17	2	2	–2
60	31.1936	31.223(3)	2.86499	2.86233	7.98	12.99	0	5	–1
61	31.2901	31.362(5)	2.85638	2.84996	7.98	10.05	0	5	1
62	31.3463		2.85138		0.16		1	3	–3
63	31.7523		2.81585		12.85		2	2	1
64	32.0214		2.79279		3.28		1	2	3
65	32.1086	32.005(4)	2.78541	2.79417	6.85	8.92	2	3	–1
66	32.1729	32.160(5)	2.77999	2.78110	2.50	12.42	2	3	0
67	32.7370	32.167(6)	2.73336	2.78049	24.84	3.25	0	0	4
68	32.7494	32.738(4)	2.73235	2.73327	0.11	3.99	1	0	–4
69	32.7494	33.009(4)	2.73235	2.71146	3.35	5.86	0	1	–4
70	32.9732		2.71432		3.35		0	1	4
71	32.9942		2.71264		0.25		1	5	0
72	33.2342		2.69359		4.59		1	4	2
73	33.3048	33.252(8)	2.68805	2.69221	22.51	11.86	2	0	2
74	33.3766	33.35(1)	2.68243	2.68417	2.00	7.91	1	1	–4
75	33.4331		2.67802		13.72		2	1	–3
76	33.7946	33.409(6)	2.65020	2.67987	0.19	6.29	1	5	–1
77	33.9568	33.46(3)	2.63791	2.67609	1.19	3.70	2	1	2
78	34.1844	34.003(5)	2.62086	2.63443	1.92	3.36	2	3	–2
79	34.1844	34.196(5)	2.62086	2.62001	0.59	7.53	0	4	–3
80	34.2044		2.61938		0.59		0	4	3
81	34.2464	34.26(1)	2.61626	2.61533	3.20	1.27	2	3	1
82	34.2464		2.61626		0.47		0	5	–2
83	34.4273		2.60293		0.47		0	5	2
84	34.4273		2.60293		0.07		0	2	–4
85	34.5003		2.59759		0.07		0	2	4
86	34.5805	34.530(3)	2.59175	2.59543	3.47	3.40	1	5	1
87	34.9592		2.56453		0.80		1	3	3
88	35.0280		2.55965		2.28		1	2	–4
89	35.2396	35.048(3)	2.54477	2.55821	11.06	7.40	2	2	–3
90	35.4289	35.234(4)	2.53160	2.54518	7.04	4.24	1	4	–3
91	35.8126	35.431(3)	2.50536	2.53142	10.12	5.28	2	2	2
92	35.8994	35.88(2)	2.49949	2.50047	2.30	2.80	1	5	–2
93	35.9782	35.96(2)	2.49420	2.49517	1.27	3.44	2	4	–1
94	36.3300		2.47085		2.33		2	4	0
95	36.9141	36.350(2)	2.43308	2.46955	3.74	5.03	0	6	0

Continuation of **Table 2**

1	2	3	4	5	6	7	8	9	10
96	37.0755	36.936(9)	2.42286	2.43172	3.51	2.04	1	0	4
97	37.0755	37.077(5)	2.42286	2.42279	2.03	4.01	0	3	–4
98	37.2484		2.41201		2.03		0	3	4
99	37.2484		2.41201		0.92		0	6	–1
100	37.4263		2.40096		0.92		0	6	1
101	37.5747		2.39181		0.16		1	1	4
102	37.6394		2.38785		0.18		1	3	–4
103	37.6594	37.656(3)	2.38663	2.38684	4.61	4.00	2	3	–3
104	37.8030		2.37789		0.06		2	4	–2
105	37.8859		2.37287		0.47		1	5	2
106	38.0165		2.36503		0.15		2	4	1
107	38.2305		2.35228		2.17		2	3	2
108	38.4007	38.226(8)	2.34224	2.35254	1.04	1.98	1	4	3
109	38.7832	38.414(8)	2.32002	2.34148	1.36	1.99	2	0	–4
110	38.8647	38.928(5)	2.31534	2.31173	0.76	2.00	1	6	0
111	38.8647		2.31534		1.43		0	5	–3
112	38.8962		2.31354		1.43		0	5	3
113	38.9281		2.31171		0.88		2	1	–4
114	39.1836		2.29723		0.89		1	2	4
115	39.4089		2.28461		0.26		1	6	–1
116	39.8126	39.406(5)	2.26237	2.28476	3.88	2.03	2	1	3
117	39.8950		2.25789		1.20		1	5	–3
118	39.8950		2.25789		0.05		0	6	–2
119	40.0240		2.25091		0.05		0	6	2
120	40.0784		2.24798		2.31		3	1	–1
121	40.1180	40.057(2)	2.24585	2.24912	12.01	6.99	3	0	0
122	40.3517		2.23338		1.25		1	6	1
123	40.4084	40.41(1)	2.23038	2.23036	0.34	4.14	2	2	–4
124	40.4797		2.22662		8.16		2	5	–1
125	40.5324	40.49(2)	2.22384	2.22605	1.12	2.03	2	5	0
126	40.5324		2.22384		0.50		0	4	–4
127	40.5566		2.22257		0.50		0	4	4
128	40.7129		2.21439		1.31		3	1	0
129	40.8493		2.20732		0.00		3	0	–2
130	40.9960	40.843(3)	2.19976	2.20762	8.32	6.87	2	2	3
131	41.0050	41.036(2)	2.19929	2.19770	0.31	8.83	1	4	–4
132	41.0050		2.19929		0.31		0	1	–5
133	41.0120		2.19893		0.31		0	1	5
134	41.0561		2.19667		6.01		1	1	–5
135	41.1851		2.19009		18.10		2	4	–3
136	41.2768		2.18544		0.08		3	1	–2
137	41.3288	41.314(3)	2.18281	2.18356	0.71	4.93	1	6	–2
138	41.4070		2.17887		5.34		1	3	4
139	41.4466		2.17688		0.21		2	4	2
140	41.9642		2.15121		0.61		3	2	–1
141	42.0079		2.14908		2.95		3	2	0
142	42.2148	41.999(8)	2.13902	2.14952	0.86	2.00	2	5	–2
143	42.4004	42.218(9)	2.13009	2.13886	1.82	1.95	2	5	1
144	42.4004		2.13009		0.08		0	2	–5

Continuation of **Table 2**

1	2	3	4	5	6	7	8	9	10
145	42.4072		2.12976		0.08		0	2	5
146	42.5300	42.407(6)	2.12389	2.12977	2.57	2.98	1	2	–5
147	42.5756	42.59(2)	2.12173	2.12098	0.40	1.02	1	5	3
148	42.6859		2.11650		1.87		3	2	–2
149	42.7304	42.720(5)	2.11440	2.11490	2.49	4.02	2	3	–4
150	43.0534		2.09928		5.46		3	1	1
151	43.1613	43.145(4)	2.09428	2.09505	0.01	3.01	1	6	2
152	43.4635		2.08042		3.64		2	3	3
153	43.4635	43.485(4)	2.08042	2.07946	1.70	3.02	0	7	–1
154	43.7329		2.06823		1.70		0	7	1
155	43.9290		2.05945		2.17		3	3	–1
156	44.0095	43.955(5)	2.05586	2.05827	0.01	2.02	3	1	–3
157	44.0095		2.05586		0.54		0	6	–3
158	44.0813		2.05268		0.54		0	6	3
159	44.2288		2.04618		0.08		3	2	1
160	44.5100		2.03391		0.91		3	3	0
161	44.6471	44.51(1)	2.02797	2.03402	3.04	3.02	1	4	4
162	44.6471	44.630(6)	2.02797	2.02870	2.04	3.92	0	3	–5
163	44.6483		2.02793		2.04		0	3	5
164	44.6483		2.02793		0.17		0	5	–4
165	44.6537		2.02769		0.17		0	5	4
166	44.8153		2.02075		6.62		1	3	–5
167	44.8208		2.02052		4.86		3	3	–2
168	44.8677	44.8(1)	2.01851	2.02047	0.06	3.01	1	7	0
169	45.0774	44.9(2)	2.00961	2.01819	3.34	1.73	1	6	–3
170	45.1331	45.15(1)	2.00726	2.00657	0.13	1.00	1	5	–4
171	45.1770		2.00541		0.35		2	5	–3
172	45.2513		2.00229		0.24		1	7	–1
173	45.3690		1.99737		0.05		3	2	–3
174	45.3884	45.493(4)	1.99656	1.99221	0.00	2.99	1	1	5
175	45.4093		1.99569		0.90		2	1	–5
176	45.4585		1.99365		0.01		2	6	–1
177	45.4742		1.99300		0.23		2	5	2
178	45.5383		1.99034		2.14		2	6	0
179	45.7910		1.97994		0.53		2	0	4
180	45.8121	45.80(1)	1.97908	1.97976	2.53	1.00	2	4	–4
181	45.8121		1.97908		0.05		0	7	–2
182	45.9292		1.97430		0.05		0	7	2
183	45.9702		1.97264		0.02		3	0	2
184	46.0117		1.97096		0.77		2	1	4
185	46.2410		1.96171		0.05		1	7	1
186	46.2629		1.96084		1.81		2	4	3
187	46.3583		1.95702		0.07		3	3	1
188	46.6592	46.285(5)	1.94510	1.95994	0.36	2.02	3	1	2
189	46.6781	46.695(3)	1.94436	1.94371	0.75	3.96	1	2	5
190	46.7828		1.94025		6.97		2	2	–5
191	46.8708		1.93681		0.58		3	4	–1
192	47.0528		1.92974		0.01		2	6	–2
193	47.0606	47.060(2)	1.92944	1.92946	7.00	5.92	1	7	–2

Continuation of **Table 2**

1	2	3	4	5	6	7	8	9	10
194	47.2477		1.92224		1.84		2	6	1
195	47.2535		1.92201		0.05		2	2	4
196	47.3501		1.91832		0.05		3	4	0
197	47.3907		1.91677		1.89		1	6	3
198	47.6224	47.398(7)	1.90798	1.91651	2.02	1.95	3	3	–3
199	47.6278	47.62(3)	1.90778	1.90816	2.29	3.07	3	0	–4
200	47.6511	47.70(2)	1.90690	1.90500	0.10	3.96	3	2	2
201	47.6511		1.90690		4.29		0	4	–5
202	47.6573		1.90667		4.29		0	4	5
203	47.8110		1.90090		0.28		1	4	–5
204	48.0399		1.89237		2.21		3	4	–2
205	48.3542	48.057(6)	1.88080	1.89173	1.80	1.97	3	1	–4
206	48.6612		1.86965		1.31		1	5	4
207	48.7320	48.664(9)	1.86710	1.86955	0.04	2.02	1	7	2
208	48.7509		1.86642		0.60		1	0	–6
209	48.7693		1.86576		3.83		1	3	5
210	49.1214	48.784(6)	1.85321	1.86525	1.22	2.93	2	3	–5
211	49.1256		1.85306		2.94		0	0	6
212	49.1424		1.85247		2.21		0	8	0
213	49.1905	49.129(2)	1.85077	1.85295	0.25		1	1	–6
214	49.2763		1.84774		0.84		3	4	1
215	49.3053		1.84672		0.03		3	2	–4
216	49.3054		1.84672		0.19		0	6	–4
217	49.3205		1.84619		0.19		0	6	4
218	49.5294		1.83889		0.38		2	3	4
219	49.5294		1.83889		0.43		0	1	–6
220	49.5325		1.83879		0.43		0	1	6
221	49.5325		1.83878		0.32		0	7	–3
222	49.5585		1.83788		0.32		0	7	3

Table 3. Interatomic distances in the crystal structure $SrCoV_2O_7$

$Atom_1$	$Atom_2$	Distance Å	$Atom_1$	$Atom_2$	Distance Å	$Atom_1$	$Atom_2$	Distance Å
1	2	3	4	5	6	7	8	9
O_1	$-Sr_4$	0.724	O_6	$-Co_1$	1.786	V_6	$-O_5$	1.569
	$-Co_4$	1.342		$-Co_4$	2.073		$-Sr_7$	1.973
	$-V_5$	1.538		$-V_7$	2.091		$-V_1$	2.046
	$-Sr_2$	1.687		$-Co_2$	2.162		$-O_8$	2.264
	$-V_2$	2.421		$-V_5$	2.373		$-O_2$	2.285
	$-V_8$	2.656		$-V_8$	2.539		$-O_9$	2.568
	$-V_7$	2.659		$-Sr_3$	2.584		$-O_4$	2.590
	$-Sr_5$	2.947		$-Sr_2$	2.791		$-O_7$	2.851
	$-O_{10}$	2.969		$-O_9$	2.932		$-V_2$	2.974
	$-Sr_7$	3.006		$-Sr_4$	2.983		$-O_8$	2.980
	$-O_9$	3.076		$-V_4$	3.018		$-Co_5$	3.043
	$-V_6$	3.106		$-O_7$	3.056		$-Co_4$	3.065
	$-O_7$	3.108		$-Co_3$	3.160		$-Sr_7$	3.092

Continuation of **Table 3**

1	2	3	4	5	6	7	8	9
	-Sr_3	3.143		-V_2	3.231		-O_1	3.106
	-O_5	3.220		-O_3	3.238		-O_4	3.387
	-Co_1	3.221		-O_{10}	3.319		-V_5	1.124
	-O_6	3.360		-V_4	3.320		-Co_4	2.063
	-Co_2	3.425		-O_1	3.360		-O_6	2.091
	-V_3	3.458		-O_1	3.485		-V_4	2.260
	-O_6	3.485		-Co_5	3.486		-O_4	2.378
	-O_7	1.387		-Sr_1	1.057		-O_{10}	2.570
	-O_5	1.696		-Sr_5	1.544		-V_1	2.574
	-Sr_6	1.975		-O_3	1.671		-O_1	2.659
	-Sr_5	2.048		-O_{10}	1.681		-Sr_5	2.814
	-V_6	2.285		-Co_1	2.151		-Sr_3	2.838
	-Co_2	2.441		-Sr_6	2.331	V_7	-V_2	2.878
O_2	-V_8	2.473		-O_9	2.813		-Sr_6	2.889
	-V_3	2.503		-O_9	3.050		-Sr_4	2.958
	-O_3	3.051		-V_3	3.091		-Co_5	2.984
	-O_9	3.065	Co_3	-V_7	3.144		-Sr_2	3.059
	-V_3	3.097		-V_1	3.157		-Co_1	3.086
	-Co_3	3.291		-O_6	3.160		-Co_3	3.144
	-Sr_4	3.493		-Co_4	3.190		-Sr_7	3.254
	-Co_1	1.561		-V_5	3.200		-Sr_1	3.276
	-Co_3	1.671		-V_2	3.228		-O_8	3.332
	-Sr_1	1.939		-O_5	3.250		-O_9	3.461
	-V_3	2.303		-O_2	3.291		-O_5	1.520
	-O_5	2.384		-O_7	3.299		-Sr_1	1.887
	-O_{10}	2.494		-Co_2	3.354		-O_{10}	2.054
	-O_9	2.817		-V_5	1.230		-Co_2	2.336
	-V_8	2.953		-O_1	1.342		-V_6	2.568
	-O_9	3.007		-Sr_4	1.927		-Co_4	2.615
O_3	-O_2	3.051		-V_2	1.933		-Sr_6	2.735
	-Sr_5	3.195		-V_7	2.063		-Co_3	2.813
	-O_6	3.238		-O_6	2.073	O_9	-O_3	2.817
	-Sr_3	3.268		-O_9	2.615		-V_1	2.847
	-V_1	3.297	Co_4	-Sr_5	2.719		-O_6	2.932
	-Co_2	3.391		-Sr_2	2.802		-O_3	3.007
	-Sr_6	3.415		-Sr_7	2.806		-Co_3	3.050
	-Sr_4	3.427		-O_{10}	2.901		-O_2	3.065
	-Sr_1	3.459		-O_4	3.036		-O_1	3.076
	-O_{10}	0.824		-V_6	3.065		-V_5	3.087
Sr_1	-Co_3	1.057		-Co_1	3.109		-O_7	3.240
	-O_9	1.887		-Co_3	3.190		-V_8	3.340

Continuation of **Table 3**

1	2	3	4	5	6	7	8	9
	-O_3	1.939		-O_5	3.215		-V_7	3.461
	-Sr_5	2.076		-O_{10}	3.350		-O_7	1.496
	-Co_1	2.519		-Co_2	3.392		-Co_2	1.598
	-O_5	2.888		-Sr_1	3.464		-Sr_5	1.958
	-V_3	2.933		-Co_2	1.092	Sr_6	-O_2	1.975
	-V_2	3.014	O_7	-O_2	1.387		-V_1	2.144
	-V_5	3.216		-V_8	1.453		-Co_3	2.331
	-Sr_6	3.249		-Sr_6	1.496		-O_9	2.735
	-V_7	3.276		-Sr_5	2.631		-V_8	2.746
	-O_3	3.459		-O_5	2.634		-V_7	2.889
	-Co_4	3.464		-V_3	2.716		-Co_5	2.903
	-Sr_4	1.448		-V_6	2.851		-O_4	3.204
	-O_1	1.687		-O_6	3.056		-V_5	3.220
	-V_8	2.007		-Co_5	3.070		-Sr_1	3.249
	-V_5	2.216		-O_1	3.108		-O_5	3.350
	-V_2	2.509		-Sr_2	3.170		-O_3	3.415
	-O_8	2.702		-Sr_3	3.219		-O_4	0.931
	-O_4	2.760		-O_9	3.240		-V_2	1.486
	-O_6	2.791		-Sr_4	3.271		-O_8	1.929
	-V_3	2.798		-Co_3	3.299		-V_6	1.973
Sr_2	-Co_4	2.802		-V_1	3.478		-Co_4	2.806
	-Sr_7	2.828		-O_4	1.485		-Sr_2	2.828
	-V_4	2.878		-Sr_7	1.486		-O_1	3.006
	-O_{10}	2.903		-Co_4	1.933		-V_4	3.087
	-Co_1	3.058		-O_{10}	2.382	Sr_7	-V_6	3.092
	-V_7	3.059		-O_1	2.421		-O_8	3.101
	-Co_2	3.158		-Sr_2	2.509		-Sr_3	3.135
	-O_7	3.170		-Sr_4	2.711		-V_1	3.159
	-Sr_3	3.345		-O_8	2.875		-Co_5	3.215
	-V_4	0.809		-V_7	2.878		-V_7	3.254
	-Co_5	1.570	V_2	-V_5	2.953		-Co_5	3.268
	-O_8	1.897		-Sr_5	2.959		-V_5	3.363
	-Co_1	2.111		-V_6	2.974		-Sr_4	3.363
	-O_6	2.584		-V_5	2.994		-O_5	3.374
Sr_3	-V_7	2.838		-Sr_1	3.014		-Sr_1	0.824
	-Sr_4	2.853		-V_3	3.118		-Co_3	1.681
	-Co_2	2.877		-Co_3	3.228	O_{10}	-O_9	2.054
	-V_1	2.958		-O_6	3.231		-Sr_5	2.341
	-Sr_7	3.135		-Sr_3	3.421		-V_2	2.382
	-O_1	3.143		-Co_1	3.449		-V_5	2.471

Continuation of **Table 3**

1	2	3	4	5	6	7	8	9
	-O_7	3.219		-Sr_3	3.460		-O_3	2.494
	-O_3	3.268		-V_4	3.475		-V_7	2.570
	-O_4	3.327		-V_8	1.717		-Co_1	2.685
	-Sr_2	3.345		-Sr_5	1.991		-V_3	2.824
	-V_2	3.421		-O_3	2.303		-Co_4	2.901
	-O_{10}	3.423		-O_2	2.503		-Sr_2	2.903
	-V_2	3.460		-O_7	2.716		-O_1	2.969
	-O_1	0.724		-Sr_2	2.798		-O_5	3.055
	-Sr_2	1.448	V_3	-O_{10}	2.824		-O_4	3.265
	-V_5	1.870		-Sr_1	2.933		-V_8	3.309
Sr_4	-Co_4	1.927		-Co_1	2.943		-O_6	3.319
	-Co_1	2.563		-Co_2	2.996		-Co_4	3.350
	-V_8	2.682		-Sr_4	3.024		-V_4	3.373
	-V_2	2.711		-Co_3	3.091		-Sr_3	3.423
	-Sr_5	2.767		-O_2	3.097		-Sr_4	3.462
	-Sr_3	2.853		-V_2	3.118		-O_7	1.453
	-V_7	2.958		-O_5	3.189		-Co_2	1.526
	-O_6	2.983		-O_1	3.458		-V_3	1.717
	-V_3	3.024		-Sr_3	0.809		-Sr_2	2.007
	-O_7	3.271		-O_8	1.529		-O_2	2.473
	-Co_2	3.352		-Co_5	1.531		-O_6	2.539
	-Sr_7	3.363		-V_7	2.260	V_8	-O_1	2.656
	-O_3	3.427		-V_1	2.344		-Sr_4	2.682
	-O_{10}	3.462		-Co_1	2.638		-Sr_6	2.746
	-V_4	3.464		-Sr_2	2.878		-O_3	2.953
	-O_2	3.493	V_4	-O_6	3.018		-O_5	3.216
	-Co_3	1.544		-Sr_7	3.087		-O_{10}	3.309
	-Sr_6	1.958		-O_4	3.220		-O_9	3.340
	-V_3	1.991		-O_6	3.320		-V_4	3.456
	-O_2	2.048		-V_5	3.340		-V_4	1.531
	-Sr_1	2.076		-O_{10}	3.373		-Sr_3	1.570
	-O_{10}	2.341		-V_8	3.456		-O_8	1.626
	-V_5	2.492		-Sr_4	3.464		-V_1	1.950
	-O_7	2.631		-V_2	3.475		-Co_2	2.879
Sr_5	-Co_4	2.719		-V_4	1.529		-Sr_6	2.903
	-Sr_4	2.767		-Co_5	1.626		-O_4	2.938
	-V_7	2.814		-Sr_3	1.897	Co_5	-V_1	2.961
	-O_1	2.947		-Sr_7	1.929		-Co_5	2.966
	-V_2	2.959		-V_1	2.007		-O_4	2.979
	-Co_2	3.174		-V_6	2.264		-V_7	2.984
	-O_3	3.195	O_8	-O_4	2.626		-V_6	3.043
	-Co_1	3.294		-Sr_2	2.702		-O_7	3.070
	-V_1	3.489		-V_2	2.875		-Sr_7	3.215
	-Co_5	1.950		-V_6	2.980		-Sr_7	3.268
V_1	-O_8	2.007		-Sr_7	3.101		-O_6	3.486
	-V_6	2.046		-O_5	3.302	O_4	-Sr_7	0.931
	-Sr_6	2.144		-V_7	3.332		-V_2	1.485

Continuation of **Table 3**

1	2	3	4	5	6	7	8	9
	-V_4	2.344		-O_4	3.342		-V_7	2.378
	-O_5	2.442		-V_7	1.124		-V_6	2.590
	-V_7	2.574		-Co_4	1.230		-O_8	2.626
	-O_9	2.847		-O_1	1.538		-V_5	2.660
	-Sr_3	2.958		-Sr_4	1.870		-Sr_2	2.760
	-Co_5	2.961		-Sr_2	2.216		-Co_5	2.938
	-Co_2	3.057		-O_6	2.373		-Co_5	2.979
	-Co_3	3.157		-O_{10}	2.471		-Co_4	3.036
	-Sr_7	3.159	V_5	-Sr_5	2.492		-V_1	3.194
	-O_4	3.194		-O_4	2.660		-Sr_6	3.204
	-O_3	3.297		-V_2	2.953		-V_4	3.220
	-O_4	3.328		-V_2	2.994		-O_{10}	3.265
	-Co_1	3.395		-O_9	3.087		-Sr_3	3.327
	-O_7	3.478		-Co_3	3.200		-V_1	3.328
	-Sr_5	3.489		-Sr_1	3.216		-O_8	3.342
	-O_3	1.561		-Sr_6	3.220		-V_6	3.387
	-O_6	1.786		-V_4	3.340		-O_9	1.520
	-Sr_3	2.111		-Sr_7	3.363		-V_6	1.569
	-Co_3	2.151		-Co_1	3.417		-O_2	1.696
	-Sr_1	2.519		-O_7	1.092		-O_3	2.384
	-Sr_4	2.563		-V_8	1.526		-V_1	2.442
	-V_4	2.638		-Sr_6	1.598		-O_7	2.634
	-O_{10}	2.685		-O_6	2.162		-Sr_1	2.888
	-V_3	2.943		-O_9	2.336		-O_{10}	3.055
	-Sr_2	3.058		-O_2	2.441		-V_3	3.189
	-V_7	3.086		-Sr_3	2.877		-Co_4	3.215
Co_1	-Co_4	3.109		-Co_5	2.879	O_5	-V_8	3.216
	-O_1	3.221	Co_2	-V_3	2.996		-O_1	3.220
	-Sr_5	3.294		-V_1	3.057		-Co_3	3.250
	-O_5	3.369		-Sr_2	3.158		-O_8	3.302
	-V_1	3.395		-Sr_5	3.174		-Sr_6	3.350
	-V_5	3.417		-Sr_4	3.352		-Co_1	3.369
	-V_2	3.449		-Co_3	3.354		-Sr_7	3.374
	-Co_2	3.488		-O_3	3.391			
				-Co_4	3.392			
				-O_1	3.425			
				-Co_1	3.488			

A separate analysis of the interatomic distances in the $SrCoV_2O_7$ structure revealed a complex coordination of atoms that ensures the stability and orderliness of the crystal lattice (Table 3). Atoms of cobalt, vanadium, strontium and oxygen participate in the formation of coordination polyhedra, which are interconnected and create a single coordination network.

The structure of $SrCoV_2O_7$ is characterized by a complex organization, where the key elements are octahedral complexes of CoO_6 and VO_6, stabilized by strontium atoms and connected through oxygen atoms (Figure). In the structure, cobalt atoms form coordination polyhedra of the CoO_6 type, where the central Co atom is surrounded by six oxygen atoms, forming octahedra. The shortest bond, Co_4-O_1 (1.342 Å), indicates a strong interaction between cobalt and oxygen, while longer bonds such as Co_1-O_6 (1.786 Å) indicate local stresses or structural deformations. Similarly, vanadium forms octahedral VO_6 complexes, where the shortest bonds, such as V_5-O_1 (1.538 Å), ensure the stability of the octahedra,

and the asymmetry of the bonds is a consequence of the influence of defects and the inter-nodal arrangement of atoms.

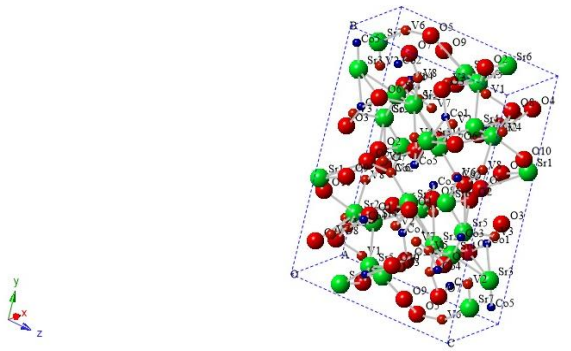

Crystal structure of $SrCoV_2O_7$ compound

Strontium atoms have a large coordination sphere and form flexible bonds with oxygen, among which Sr_4-O_1 (0.724 Å) is the most pronounced. These bonds stabilize the three-dimensional network formed by the CoO_6 and VO_6 octahedra, filling the gaps between them. The oxygen in the structure plays a critical role in ensuring the bonding of the octahedra and lattice stability. For instance, the O_7-Co_2 (1.092 Å) and O_7-V_8 (1.453 Å) bonds demonstrate their importance for the overall strength of the material. At the same time, oxygen also affects the electron density, regulating the conductivity and magnetic properties of the material[11, 12].

Microstructural defects are observed in the structure, which significantly affect its physical and chemical properties. Vacancies caused by the absence of atoms in the lattice nodes can reduce strength and stability. The inter-nodal arrangement of atoms, which is typical for materials synthesized at high temperatures, leads to local symmetry distortions[13–15]. Temperature effects during synthesis or sintering contribute to the fluctuations of atoms, which can move from their nodal positions, creating additional defects[16]. For example, differences in the values of diffraction planes, such as for the (0, 4, 2) plane with d=3.084 Å, indicate an uneven arrangement of atoms in the structure.

All these factors provide a unique organization of $SrCoV_2O_7$ that balances stability and functionality. The three-dimensional network of CoO_6 and VO_6 octahedra stabilized by strontium atoms allows the material to demonstrate promising properties for use in high-temperature ceramics, electronic devices and catalysts. The interaction between the octahedra through oxygen atoms ensures stability, while structural defects contribute to the material's adaptation to changing conditions[17, 18].

Defects in the crystal structure, such as vacancies and inter-nodal arrangement of atoms, play an important role in the formation of the properties of $SrCoV_2O_7$ material. The study demonstrated that the structure of the complex is characterized by the partial filling of the lattice nodes, which is confirmed by the analysis of diffraction data for the (0, 4, 2) planes with an interplanar distance of d=3.084 Å. Defects are formed during the synthesis of the material due to temperature effects and imperfect coordination of CoO_6 and VO_6 polyhedra, which affects the functional properties of the material[19]. The presence of vacancies, for example, in oxygen nodes, breaks the symmetry of the crystal structure and weakens the bonds in the octahedra, which reduces the mechanical strength of the material[20–22]. The structure analysis showed that the Co_1-O_3 (1.561 Å) and Co_1-O_6 (1.786 Å) bonds are longer than expected, which is due to local deformations due to vacancies. Such changes are particularly important for materials used in high-temperature environments or under mechanical stress.

The electrical conductivity of the material under study also depends largely on defects. For example, the inter-nodal arrangement of oxygen atoms creates potential barriers to the movement of electrons along polyhedron chains[23]. In areas of local deformation, such as in the V_2-O_4 bonds (1.485 Å), the electron density decreases, which limits the effective charge transport and affects the control of conductivity in oxide materials for electronics.

The thermal conductivity of the structure decreases due to irregularities in the lattice caused by defects. The vacuum spaces in the nodes and the inter-node arrangement of atoms prevent phonon propagation[24]. For example, the displacement of oxygen atoms forming the O_7-Co_2 (1.092 Å) and O_7-V_8 (1.453 Å) bonds creates local barriers to heat waves. Such effects can be useful for applications where thermal conductivity needs to be reduced, such as in insulating materials.

The temperature stability of a material also depends on defects. During synthesis, high temperatures promote atomic fluctuations, which increase the number of vacancies or move atoms to inter-node positions[25]. These processes reduce the overall stability of the structure. During the experiment, the expansion of some octahedra due to local temperature stresses was observed, indicating a decrease in the regularity of the coordination geometry.

The $SrCoV_2O_7$ compound exhibits unique structural and physicochemical properties that make it promising for use in high-tech industries. Thanks to its partial ionic conductivity due to structural defects, the material can be used to create components for ionic conductors, sensors and fuel cell elements[26]. Its stable structure and low thermal conductivity open opportunities for use in ULTCC, which is substantial for the

development of multilayer microelectronic devices. In addition, the activity of CoO_6 and VO_6 coordination polymers in redox processes allows the material to be used as a catalyst in chemical reactions where structural defects serve as additional active sites, increasing catalytic efficiency.

Thus, a detailed analysis of the defects in the crystal structure of $SrCoV_2O_7$ has shown that they significantly affect the mechanical, electrical, and thermal properties of the material. Despite the presence of structural defects, the calculated and experimental data obtained confirm the stability of the model and the high potential of the material for use in electronics, ceramic technology, and catalysis. An important role in this is played by the strong bonds between the coordination polyhedra and the presence of structural flexibility, which allows the material to adapt to different operating conditions.

In this study, the crystal structure and microstructural characteristics of $SrCoV_2O_7$ ceramics, which is a potential material for microwave technologies, were investigated. According to XRD data, the produced single-phase material is consistent with the known literature results, confirming its high phase purity and the efficiency of the synthesis method used. Structural characteristics, including crystal lattice parameters, demonstrate excellent agreement with the literature data.

The results obtained can be compared with similar scientific works, where various microwave dielectric materials fabricated by low-temperature sintering have demonstrated attractive characteristics for ULTCC applications. For example, the study by Sun *et al.*[27] showed that $Bi_6B_{10}O_{24}$ ceramics with the addition of 0.1 mol B_2O_3 were sintered at 710 °C and had excellent microwave properties with εr=12.5 and $Q\times f$=38.200 GHz. This is similar to the results for the ceramics under study, where crystal structure stability is an important factor in achieving optimal performance.

Regarding the properties similar to the microwave dielectric characteristics of $SrCoV_2O_7$, it is worth noting the work of Shuzhao *et al.*[28], where the Na_2O-Bi_2O_3-MoO_3 system was studied and it was shown that such ceramics have excellent dielectric properties when sintered at temperatures below 750 °C. Comparing these results, it can be noted that low-temperature sintering and structural stability are important for achieving high material performance. In addition, Zang *et al.*[29] studied $CaMoO_4$ ceramics sintered at 600 °C. This ceramic also demonstrated good dielectric properties, which correlate with the results obtained in this study. In the context of crystal structure stability and phase purity, the results of this work and previous scientific data confirm the importance of careful control of synthesis and sintering conditions to achieve high microwave performance. Similarly, other studies, such as the work of Li *et al.*[30] show how precise control of the sintering composition and temperature can significantly improve the dielectric properties of the material, which also confirms the importance of optimizing the synthesis process.

As for the comparison of the results with other ceramic materials, it is possible to note that $SrCoV_2O_7$ ceramics show certain differences in characteristics. This material has a stable crystal structure and high $Q\times f$ parameters compared to other materials, such as $Zn_3B_2O_6$, $Ag_2SrV_4O_{12}$, and $Li_4Mo_5O_{17}$, *etc*. The paper by Yoon *et al.*[31] shows that $Ba_3V_4O_{13}$-BaV_2O_6 ceramics have good microwave properties and high chemical compatibility, and $Zn_3B_2O_6$ obtained by Li *et al.*[32] in a two-step sintering process has a good density, but their dielectric and microwave properties are not as high as those of $SrCoV_2O_7$. Furthermore, lithium molybdate $Li_4Mo_5O_{17}$, as shown by Khan *et al.*[33], has high dielectric properties, but its characteristics may be influenced by the polaron model, which makes it less stable. Compared to ZnO-SiO_2-B_2O_3-based composites in the work of Olszewska-Placha *et al.*[34], $SrCoV_2O_7$ also shows greater stability, which is important for applications in high-precision microwave components.

$SrCoV_2O_7$ ceramics are notable for their stability at high temperatures and high phase purity, which makes them a promising material for microwave technologies, in particular in comparison with such materials as $BaMg_{2-x}Zn_xV_2O_8$, $Li_8Mg_xTi_3O_{9+x}F_2$, and Li_2WO_4. Zhai *et al.*[35] showed that $Li_8Mg_5Ti_3O_{14}F_2$ ceramics has good microwave properties, but its thermal stability is significantly inferior to that of $SrCoV_2O_7$. In addition, the results of Ding *et al.*[36] also indicate a good potential for improving the thermal stability of the studied ceramics. Other studies by Szwagierczak *et al.*[37] such as the development of Li_2WO_4-based substrates also demonstrate low dielectric losses and good stability at terahertz frequencies compared to $SrCoV_2O_7$.

According to the study of Unnimaya *et al.*[38], $Mg_4V_2O_9$ ceramics demonstrate high efficiency in the microwave range, as well as good chemical compatibility, which makes it promising for use in the design of terahertz antenna array fairings. This study can serve as an example for comparison with the material under study, as it has significantly better stability at high temperatures, which allows it to be used in microwave technologies in a wider range of conditions. Another work carried out by Zhou *et al.*[39] showed that microwave dielectric ceramics $(1–x)BiVO_{4-x}TiO_2$ (x=0.4, 0.5, 0.55, and 0.6), produced by low-temperature firing by the traditional solid-phase reaction method, also has good microwave properties.

In summary, the results of the study of $SrCoV_2O_7$ ceramics show the great potential of this material for use in microwave technologies due to its stable crystal

structure and high phase purity[40, 41]. However, it is also worth noting the environmental aspect. Compared to $SrCoV_2O_7$, borosilicate glasses have a higher sintering temperature, but their environmental properties allow them to be used in cost-effective and sustainable processes. Given these advantages, $SrCoV_2O_7$ ceramics, due to their stability at lower sintering temperatures, may also be promising for use in environmentally friendly microwave technologies. Further research aimed at studying atomic arrangement defects and improving dielectric and magnetic properties may further improve the characteristics of this material for future applications in high-precision components.

4. Conclusions

The study of the crystal structure of $SrCoV_2O_7$ ceramics confirmed the preparation of a single-phase material with characteristics that are in good agreement with known literature data. The diffraction spectrum of the synthesized sample fully corresponds to the spectrum of the compound from the ICDD PDF database No. 00-044-0455, which confirms the high phase purity of the material and the efficiency of the applied synthesis methodology. The $SrCoV_2O_7$ ceramic crystallizes in monoclinic syngony with the P121/c1(14) space group of symmetry, and the lattice parameters are as follows: a=6.8360(7) Å, b=14.823(2) Å, c=11.271(1) Å, and angle β=99.4610(5)° show excellent agreement with known data, confirming the correctness of the synthesis and the chosen conditions.

The proposed structural model of $SrCoV_2O_7$ addresses microstructural parameters and details the internal structure of the material. Particular attention is drawn to the problem of incomplete filling of the ideal point system in the structural model. Such anomalies may be associated with defects in the atomic arrangement arising from the specifics of the synthesis and sintering processes. The study of these defects demonstrates the behaviour of the material at the atomic level and assesses their impact on functional properties, on magnetic and dielectric characteristics.

These results highlight the importance of precise control of the synthesis conditions, such as sintering temperature, holding time, and quality and purity of the starting reagents. Carefully selected conditions ensure the formation of a stable crystal structure and high-performance characteristics. Thus, the study significantly contributed to the study of the crystal structure and microstructure of $SrCoV_2O_7$, which can be the basis for further research on the physical and chemical properties of this material. The data obtained during the study contribute to the promising use of $SrCoV_2O_7$ in functional ceramics for modern microwave technologies, in the manufacture of multilayer components such as resonators, filters, or antennas. The obtained results confirm that $SrCoV_2O_7$ ceramics is a promising material for use in modern microwave technologies due to the combination of crystal structure stability and high phase purity. Further research aimed at studying the magnetic and dielectric properties of this material can expand its functionality and open up new opportunities for practical applications.

References

[1] Ahmed, A. M.; Hasan, S. A.; Majeed, S. A. 5G Mobile Systems, Challenges and Technologies: A Survey. *J. Theor. Appl. Inf. Technol.* **2019**, *97*, 3214–3226.

[2] Varghese, J.; Ramachandran, P.; Sobocinski, M.; Vahera, T.; Jantunen, H. ULTCC Glass Composites Based on Rutile and Anatase with Cofiring at 400°C for High Frequency Applications. *ACS Sustain. Chem. Eng.* **2019**, *7*, 4274–4283. https://doi.org/10.1021/acssuschemeng.8b06048

[3] Liu, J.; Liu, B.; Hu, C.; Zhou, Q.; Song, K. Ultra-Low Temperature Sintered (1-x)BaV_2O_6-xLiF Ceramics for ULTCC and 5G Millimeter-Wave Antenna Applications. *J. Eur. Ceram. Soc.* **2023**, *43*, 6130–6136. https://doi.org/10.1016/j.jeurceramsoc.2023.07.006

[4] Deng, Y.; Yao, P.; Li, B. A Novel Ultra-Low Temperature Sintered Li_2CO_3 Doped $Ba_3V_2O_8$ Microwave Ceramics. *Mater. Lett.* **2021**, *285*, 129125. https://doi.org/10.1016/j.matlet.2020.129125

[5] Huang, C.L.; Chiang, P.E.; Hsu, T.H. Effect of a Minute Substitution on the Structure and Microwave Dielectric Properties of Novel $LiCoVO_4$ Ceramics for ULTCC Applications. *J. Asian Ceramic Soc.* **2021**, *9*, 1154–1164. https://doi.org/10.1080/21870764.2021.1945746

[6] Suresh, E.; Ratheesh, R. Structure and Microwave Dielectric Properties of Glass Free Low Temperature Co-Firable $SrMV_2O_7$ (M= Mg, Zn) Ceramics. *J. Alloys Compd.* **2019**, *808*, 151641. https://doi.org/10.1016/j.jallcom.2019.07.353

[7] Huang, C.-L.; Huang, J.-L.; Tsai, M.-H. Ultra-Low Temperature Sintering and Temperature Stable Microwave Dielectrics of $(Mg_{1-x}Zn_x)V_2O_6$ (x=0-0.09) Ceramics. *J. Asian Ceramic Soc.* **2021**, *9*, 106–112. https://doi.org/10.1080/21870764.2020.1848037

[8] Zou, A.; Gao, W.; Mu, Y.; Li, L.; Wang, J.; Han, J. Microwave Dielectric Properties of a Novel Li_2O-Al_2O_3-B_2O_3 Glass-Ceramic for ULTCC Application. *Ceram. Int.* **2023**, *49*, 35274–35284. https://doi.org/10.1016/j.ceramint.2023.08.200

[9] Yu, M.; Tang, Y.; Li, J.; Fang, W.; Duan, L.; Fang, L. Microwave Dielectric Properties and Chemical Compatibility with Alumina Electrode of Two Novel Ultra-Low Temperature Firing $ATeMoO_6$ (A=Mg, Zn) Ceramics. *Ceram. Int.* **2020**, *46*, 25619–25625. https://doi.org/10.1016/j.ceramint.2020.07.036

[10] Huang, Y.-T.; Huang, C.-C.; Hsu, T.-H.; Huang, C.-L. Ultra-Low Temperature Sintering and Microwave Dielectric Properties of Mg-Substituted $SrCoV_2O_7$ Ceramics. *J. Asian Ceramic Soc.* **2022**, *10*, 188–195. https://doi.org/10.1080/21870764.2022.2031535

[11] Bondarenko, I. N.; Gorbenko, E. A.; Krasnoshchok, V. I. Microwave Switch Based on a Waveguide T-Junction for a Compression Resonant Pulse Former. *Telecommun. Radio Eng.* **2017**, *76*, 469–475. https://doi.org/10.1615/TelecomRadEng.v76.i6.20

[12] Bondarenko, I.; Galich, A. Resonant Irregular Hybrid Structures. *2016 13th International Conference on Modern Problems of Radio Engineering, Telecommunications and Computer Science (TCSET)* **2016**, *1*, 183–185. https://doi.org/10.1109/TCSET.2016.7452007
[13] Grigorenko, G. M.; Adeeva, L. I.; Tunik, A. Y.; Korzhik, V. N.; Doroshenko, L. K.; Titkov, Y. P.; Chaika, A. A. Structurization of Coatings in the Plasma Arc Spraying Process Using B4C + (Cr, Fe)(7)C-3-Cored Wires. *Powder Metall Met Ceram.* **2019**, *58*, 312–322. https://doi.org/10.1007/s11106-019-00080-1
[14] Grigorenko, G. M.; Adeeva, L. I.; Tunik, A. Y.; Korzhik, V. N.; Karpets, M. V. Plasma Arc Coatings Produced from Powder-Cored Wires with Steel Sheaths. *Powder Metall. Met. Ceram.* **2020**, *59*, 318–329. https://doi.org/10.1007/s11106-020-00165-2
[15] Han, J.; Shi, Y.; Guo, J. C.; Volodymyr, K.; Le, W. Y.; Dai, F. X. Porosity Inhibition of Aluminum Alloy by Power-Modulated Laser Welding and Mechanism Analysis. *J. Manufact. Proces.* **2023**, *102*, 827–838. https://doi.org/10.1016/j.jmapro.2023.08.001
[16] Montayev, S. A.; Ristavletov, R. A.; Omarov, B. A.; Dosov, K. Z.; Usenkulov, Z. A. Use of Granulated Metallurgy Slag in the Raw Mix for Producing Ceramic Paving Stones: Insights from an Experiment in Kazakhstan. *ISVS e-journal* **2023**, *10*, 91–105.
[17] Khardazi, S.; Zaitouni, H.; Neqali, A.; Mezzane, D.; Amjoud, M.; Abkhar, Z.; Lyubchyk, S.; Rožič, B.; Kutnjak, Z.; Lukyanchuk, I. Enhancement of the Electrocaloric Effect in the 0.4BCZT-0.6BTSn Ceramic Synthesized by Sol-Gel Route. *Mater. Res. Expr.* **2023**, *10*, 125509. https://doi.org/10.1088/2053-1591/ad1773
[18] Khardazi, S.; Zaitouni, H.; Neqali, A.; Lyubchyk, S.; Mezzane, D.; Amjoud, M.; Choukri, E.; Kutnjak, Z. Enhanced Thermal Stability of Dielectric and Energy Storage Properties in 0.4BCZT-0.6BTSn Lead-Free Ceramics Elaborated by Sol-Gel Method. *J. Phys. Chem. Sol.* **2023**, *177*, 111302. https://doi.org/10.1016/j.jpcs.2023.111302
[19] Luniov, S. V. Calculation of Electron Mobility for the Strained Germanium Nanofilm. *J. Nano- Electron. Phys.* **2019**, *11*, 02023. https://doi.org/10.21272/jnep.11(2).02023
[20] Feng, X. D.; Shi, Y.; Zhang, W. Z.; Korzhyk, V. Hydrogen Embrittlement Failure Behavior of Fatigue-Damaged Welded TC4 Alloy Joints. *Crystals* **2023**, *13*, 512. https://doi.org/10.3390/cryst13030512
[21] Sydorchuk, P.; Khlyap, G.; Andrukhiv, A. Growth and Some Properties of Heterostructures Based on New Narrow-Gap Semiconductor ZnCdHgTe. *Cryst. Res. Technol.* **2001**, *36*, 361–369. https://doi.org/10.1002/1521-4079(200106)36:4/5<361::AID-CRAT361>3.0.CO;2-5
[22] Nemoshkalenko, V. V.; Borisenko, S. V.; Uvarov, V. N.; Yaresko, A. N.; Vakhney, A. G.; Senkevich, A. I.; Borisenko, T. N.; Borisenko, V. D. Electronic Structure of the R2Ti2O7 (*R* =*S m-Er*, Yb, Lu) Oxides. *Physic. Rev. B* **2001**, *63*, 075106. https://doi.org/10.1103/PhysRevB.63.075106
[23] Tuan, P. L.; Kulik, M.; Stef, M.; Phuc, T. V.; My, N. T. B.; Zelenyak, T. Y.; Buse, G.; Racu, A.; Doroshkevich, A.; Khiem, L. H.; *et al*. An Examination on the Porosity of ErF_3 Doped CaF_2 Crystal Using the Rutherford Back-Scattering Method. *Nucl. Instrum. Methods Phys. Res. B: Beam Interact. Mater. At.* **2024**, *547*, 165178. https://doi.org/10.1016/j.nimb.2023.165178
[24] Bacherikov, Y. Yu.; Okhrimenko, O. B.; Pekur, D. V.; Ponomarenko, V. V.; Sadigov, A.; Lyubchyk, S. B.; Lyubchyk, S. I. Multifunctional Spectrophotometric Sensor Based on Photosensitive Capacitor. *Semicond. Phys. Quantum Electron. Optoelectron.* **2024**, *27*, 495–501. https://doi.org/10.15407/spqeo27.04.495
[25] Bondarenko, I. N.; Vasiliev, Yu. S.; Zhizhiriy, A. S.; Ishenko, A. L. Arrangement Device for Monitoring of Parameters of Microwave Resonators. In *2010 20th International Crimean Conference "Microwave & Telecommunication Technology"*; 13–17 Sept. 2010; pp. 969–970. https://doi.org/10.1109/crmico.2010.5632420
[26] Dai, Z. C.; Tan, M.; Yang, Y.; Liu, X.; Wang, R.; Su, Y. X. Massive Coordination of Distributed Energy Resources in VPP: A Mean Field RL-Based Bi-Level Optimization Approach. *IEEE Trans. Cybern.* **2025**, *55*, 1332–1346. https://doi.org/10.1109/TCYB.2024.3525121
[27] Sun, S.; Zhang, Q.; Dai, Y.; Pei, X. Enhanced Microwave Dielectric Properties of $Bi_6B_{10}O_{24}$ Ceramics as Ultra-Low Temperature Co-Fired Ceramics Materials. *J. Mater. Sci. Mater. Electron.* **2022**, *33*, 13604–13613. https://doi.org/10.1007/s10854-022-08295-6
[28] Shuzhao, H.; Zhou, D.; Pang, L.; Dang, M.-Z.; Sun, S.-K.; Zhou, T.; Trukhanov, S.; Trukhanov, A.; Sombra, S.; Li, Q.; *et al*. Ultra-Low Temperature Co-Fired Ceramics with Adjustable Microwave Dielectric Properties in Na_2O-Bi_2O_3-MoO_3 Ternary System: A Comprehensive Study. *J. Mater. Chem. C Mater.* **2022**, *10*, 2008–2016. https://doi.org/10.1039/D1TC05557G
[29] Zang, M.; Zheng, M.; Zhu, M.; Hou, Y. Low-Temperature Sintering and Microwave Dielectric Properties of $CaMoO_4$ Ceramics for LTCC and ULTCC Applications. *J. Eur. Ceram. Soc.* **2023**, *44*, 293–301. https://doi.org/10.1016/j.jeurceramsoc.2023.09.029
[30] Li, F.; Li, Y.-X.; Li, Y.; Feng, X.; Zhang, J.; Liu, X.; Lu, Y.; Wang, S.; Liao, Y.; Tang, T.; *et al*. Enhanced Na+-Substituted $Li_2Mg_2Mo_3O_{12}$ Ceramic Substrate Based on Ultra-Low Temperature Co-Fired Ceramic Technology for Microwave and Terahertz Polarization-Selective Functions. *J. Eur. Ceram. Soc.* **2022**, *43*, 384–391. https://doi.org/10.1016/j.jeurceramsoc.2022.10.031
[31] Yoon, S. O.; Hong, S.; Cho, H.-H.; Kim, S. Microwave Dielectric Properties of Ultra-Low Temperature Co-Firable Ba_3V_4O13-BaV_2O_6 Ceramics. *J. Korean Inst. Electr. Electronic Mater. Eng.* **2021**, *34*, 342–347. https://doi.org/10.4313/JKEM.2021.34.5.342
[32] Li, C.; Liu, Y.; Chi, M.; Luo, X.; Liu, B.; Mao, M.; Barzegar-Bafrooei, H.; Wang, G.; Taheri-Nassaj, E.; Song, K. ULTCC Post-Annealing Cold Sintering Densification Process, Microwave Dielectric Properties of $Zn_3B_2O_6$ Ceramics. *Mater. Today. Commun.* **2022**, *33*, 104997. https://doi.org/10.1016/j.mtcomm.2022.104997
[33] Khan, R.; Khan, I.; Ali, B.; Muhammad, R.; Samad, A.; Shah, A.; Song, K.; Wang, D. Structural, Dielectric, Optical, and Electrochemical Performance of $Li_4Mo_5O_{17}$ for ULTCC Applications. *Mater. Res. Bull.* **2022**, *160*, 112142. https://doi.org/10.1016/j.materresbull.2022.112142
[34] Olszewska-Placha, M.; Varghese, J.; Szwagierczak, D.; Birgit, M.; Ziesche, S.; Rudnicki, J.; Synkiewicz-Musialska, B. Bulk Glass-Ceramic Composites and ULTCC Substrates for Microwave and Millimetre-Wave Applications. *Mater. Res. Bull.* **2024**, *177*, 112862. https://doi.org/10.1016/j.materresbull.2024.112862
[35] Zhai, S.; Liu, P.; Wu, S. Novel Ultra-Low Loss and Low-Fired $Li_8Mg_xTi_3O_{9+x}F_2$ Microwave Dielectric Ceramics for Resonator Antenna Applications. *J. Eur. Ceram. Soc.* **2023**, *43*, 3331–3337. https://doi.org/10.1016/j.jeurceramsoc.2023.01.041
[36] Ding, L.; Heng, B.; Feng, X.; Bian, W.; Zhu, H.; Wang, L.; Hou, Y.; Zhang, Q. One-Step Synthesis of $Li_2Mg_2Mo_3O_{12}$-$(Li_{1/2}Bi_{1/2})MoO_4$ Composite Ceramics with a Stable Temperature Coefficient for ULTCC Applications. *J. Mater. Sci. Mater. Electron.* **2024**, *35*, 908. https://doi.org/10.1007/s10854-024-12647-9
[37] Szwagierczak, D.; Synkiewicz-Musialska, B.; Kulawik, J.; Czerwińska, E.; Pałka, N. Ultra-Low Temperature Cofired Ceramics

Based on Li_2WO_4 as Perspective Substrate Materials for Terahertz Frequencies. *J. Adv. Ceram.* **2023**, *12*, 526–538. https://doi.org/10.26599/JAC.2023.9220701
[38] Unnimaya, A. N.; Suresh, E. K.; Ratheesh, R. Crystal Structure and Microwave Dielectric Properties of New Alkaline Earth Vanadate $A_4V_2O_9$ (A=Ba, Sr, Ca, Mg and Zn) Ceramics for LTCC Applications. *Mater. Res. Bull.* **2017**, *88*, 174–181. https://doi.org/10.1016/j.materresbull.2016.12.026
[39] Zhou, D.; Guo, D.; Li, W.-B.; Pang, L.-X.; Yao, X.; Wang, D.-W.; Reaney, I. M. Novel Temperature Stable High-ε_r Microwave Dielectrics in the Bi_2O_3-TiO_2-V_2O_5 System. *J. Mater. Chem. C* **2016**, *4*, 5357–5362. https://doi.org/10.1039/C6TC01431C
[40] Savvova, O.; Shymon, V.; Fesenko, O.; Babich, O.; Alfeldii, S. Development of Strengthened Bioactive Calcium Phosphate-Silicate Glass Ceramics for Bone Implants. *Chem. Chem. Technol.* **2020**, *14*, 109–115. https://doi.org/10.23939/chcht14.01.109
[41] Zelenskii, O.; Shmalko, V.; Panov, E.; Shylovych, T.; Shylovych, Y.; Rudkevich, M. Modification of Ceramics and Ceramic Glazers with Carbon Nanoadditives, and Properties of the Modified Materials. *Chem. Chem. Technol.* **2019**, *13*, 247–253. https://doi.org/10.23939/chcht13.02.247

Received: March 28, 2025 / Revised: April 12, 2025 / Accepted: April 25, 2025

КРИСТАЛІЧНА СТРУКТУРА ТА ВЛАСТИВОСТІ КЕРАМІКИ НА ОСНОВІ ВАНАДАТУ СТРОНЦІЮ І КОБАЛЬТУ ДЛЯ МІКРОХВИЛЬОВОГО ЗАСТОСУВАННЯ

Анотація. *Для розроблення стільникового зв'язку нового покоління потрібні матеріали з належними діелектричними властивостями на високих частотах. Характеристики кераміки $SrCoV_2O_7$, синтезованої за технологією ультранизькотемпературної спільно обпаленої кераміки (ULTCC), перспективні. У дослідженні проаналізовано кристалічну структуру цієї кераміки за допомогою дифракції рентгенівських променів, SEM мікроскопії й енергодисперсійної спектроскопії. Результати підтвердили однофазну моноклінну структуру (P 1 21/c 1) із параметрами решітки a=6,8360(7) Å, b=14,823(2) Å, c=11,271(1) Å, β=99,4610(5)°. Завдяки діелектричним властивостям і сумісності із алюмінієвими електродами матеріал демонструє потенціал для мікрохвильових застосувань, зокрема для резонаторів, антен та фільтрів.*

Ключові слова: *оглядова геометрія Брег – Брентано, метод Рітвельда, низькотемпературний синтез, теплопровідність, діелектрики, спікання.*